JCI The Journal of Clinical Investigation

PKCθ promotes c-Rel–driven mammary tumorigenesis in mice and humans by repressing estrogen receptor α synthesis

Karine Belguise, Gail E. Sonenshein

J Clin Invest. 2007;117(12):4009-4021. https://doi.org/10.1172/JCI32424.

Research Article **Oncology**

The vast majority of primary human breast cancer tissues display aberrant nuclear NF-κB c-Rel expression. A causal role for c-Rel in mammary tumorigenesis has been demonstrated using a c-Rel transgenic mouse model; however, tumors developed with a long latency, suggesting a second event is needed to trigger tumorigenesis. Here we show that c-Rel activity in the mammary gland is repressed by estrogen receptor α (ERα) signaling, and we identify an epigenetic mechanism in breast cancer mediated by activation of what we believe is a novel PKCθ-Akt pathway that leads to downregulation of ERα synthesis and derepression of c-Rel. ERα levels were lower in c-Rel–induced mammary tumors compared with normal mammary gland tissue. PKCθ induced c-Rel activity and target gene expression and promoted growth of c-Rel- and c-RelxCK2α–driven mouse mammary tumor–derived cell lines. RNA expression levels of *PKC*θ and c-Rel target genes were inversely correlated with *ER*α levels in human breast cancer specimens. PKCθ activated Akt, thereby inactivating forkhead box O protein 3a (FOXO3a) and leading to decreased synthesis of its target genes, *ER*α and $p27^{Kip1}$. Thus we have shown that activation of PKCθ inhibits the FOXO3a/ERα/$p27^{Kip1}$ axis that normally maintains an epithelial cell phenotype and induces c-Rel target genes, thereby promoting proliferation, survival, and more invasive breast cancer.

PKCθ promotes c-Rel–driven mammary tumorigenesis in mice and humans by repressing estrogen receptor α synthesis

Karine Belguise and Gail E. Sonenshein

Department of Biochemistry and Women's Health Interdisciplinary Research Center, Boston University School of Medicine, Boston, Massachusetts, USA.

The vast majority of primary human breast cancer tissues display aberrant nuclear NF-κB c-Rel expression. A causal role for c-Rel in mammary tumorigenesis has been demonstrated using a c-Rel transgenic mouse model; however, tumors developed with a long latency, suggesting a second event is needed to trigger tumorigenesis. Here we show that c-Rel activity in the mammary gland is repressed by estrogen receptor α (ERα) signaling, and we identify an epigenetic mechanism in breast cancer mediated by activation of what we believe is a novel PKCθ-Akt pathway that leads to downregulation of ERα synthesis and derepression of c-Rel. ERα levels were lower in c-Rel–induced mammary tumors compared with normal mammary gland tissue. PKCθ induced c-Rel activity and target gene expression and promoted growth of c-Rel- and c-RelxCK2α–driven mouse mammary tumor–derived cell lines. RNA expression levels of *PKC*θ and c-Rel target genes were inversely correlated with *ER*α levels in human breast cancer specimens. PKCθ activated Akt, thereby inactivating forkhead box O protein 3a (FOXO3a) and leading to decreased synthesis of its target genes, *ER*α and *p27^{Kip1}*. Thus we have shown that activation of PKCθ inhibits the FOXO3a/ERα/p27^{Kip1} axis that normally maintains an epithelial cell phenotype and induces c-Rel target genes, thereby promoting proliferation, survival, and more invasive breast cancer.

Introduction

The c-Rel transcription factor is a member of the Rel/NF-κB family, which also includes RelA, RelB, p50, and p52. These proteins are related through a highly conserved N-terminal region termed the Rel homology domain, which is responsible for DNA binding, dimerization, nuclear localization, and inhibitor of NF-κB (IκB) binding (1). Overexpression, amplification, or rearrangement of the *c-REL* gene has been reported in solid (2) as well as hematopoietic malignancies (3). Approximately 85% of primary human breast cancer tissue samples aberrantly express high levels of nuclear c-Rel (2, 4). The ability of c-Rel to transform in vivo has been demonstrated, as approximately 32% of transgenic mice with c-*Rel* under the control of the mouse mammary tumor virus (MMTV) long-terminal repeat promoter developed 1 or more mammary tumors at an average age of 19.9 months (5). The long latency led us to postulate that a second event was required. CK2, a ubiquitously expressed serine/threonine kinase, has been shown to enhance NF-κB activity and transform the phenotype of breast cancer cells in vitro (6). Transgenic mice expressing the catalytic CK2α subunit under the control of the MMTV promoter developed late onset mammary tumors in approximately 30% of animals (7). We recently prepared a bitransgenic MMTV–c-*RelxCK2*α mouse model. While the percentage of mice developing mammary tumors increased, the average age of onset in the bitransgenic animals was again late (20.8 months) (8). Of note, c-Rel DNA binding in extracts from mammary glands of MMTV–*c-Rel* or MMTV–*c-RelxCK2*α animals was relatively weak compared with equivalent amounts of c-Rel detected in extracts from WEHI 231 B lymphoma cells (ref. 5 and data not shown). These data suggest the hypothesis that a factor present in mammary tissue can inhibit c-Rel activity and thereby delay tumor formation by this NF-κB subunit.

The intracellular estrogen receptor α (ERα) regulates the normal physiology of the mammary gland and breast cancer development. Upon binding of its ligand, the steroid hormone estrogen or 17β-estradiol (E2), the E2/ERα complex interacts with specific estrogen response elements (EREs) located in the promoter regions of target genes and activates gene transcription. In addition to this classic mechanism, the E2/ERα complex can also regulate the expression of target genes without DNA binding by interacting with other transcription factors, including NF-κB (9). Several mechanisms of mutually antagonistic cross-talk between the NF-κB and ERα signaling pathways have been identified: (a) direct interaction between ERα and NF-κB subunits, leading either to inhibition of NF-κB DNA binding or to transcriptional interference of DNA-bound NF-κB; (b) competition for a common coactivator; (c) induction of IκBα level, resulting in sequestration of NF-κB in the cytoplasm; and (d) inhibition of de novo RelB synthesis by ERα (10, 11).

Elevated PKC activity has been reported in malignant breast tissues compared with normal tissues (12, 13). The PKCs are serine/threonine protein kinases, and 11 closely related PKC isoforms have been described, which have been grouped into 3 subfamilies based on their structure and ability to respond to calcium and/or diacylglycerol (DAG). These include the conventional (α, βI, βII, and γ), novel (δ, ε, θ, and η), and atypical (ζ and λ/τ) PKC isoforms

Nonstandard abbreviations used: CKI, cyclin-dependent kinase inhibitor; DAG, diacylglycerol; E2, 17β-estradiol; EGCG, epigallocatechin-3-gallate; ERα, estrogen receptor α; ERE, estrogen response element; EV, empty vector; FOXO3a, forkhead box O protein 3a; IκB, inhibitor of NF-κB; IKK, IκB kinase; MMTV, mouse mammary tumor virus; ONP, oligonucleotide precipitation; p27, p27^{Kip1}; PKCθ-A/E, constitutively active PKCθ; PKCθ-K/R, kinase-defective PKCθ; PR, progesterone receptor; RARα, retinoic acid receptor α; WCE, whole cell extract.

Conflict of interest: The authors have declared that no conflict of interest exists.

Citation for this article: *J. Clin. Invest.* **117**:4009–4021 (2007). doi:10.1172/JCI32424.

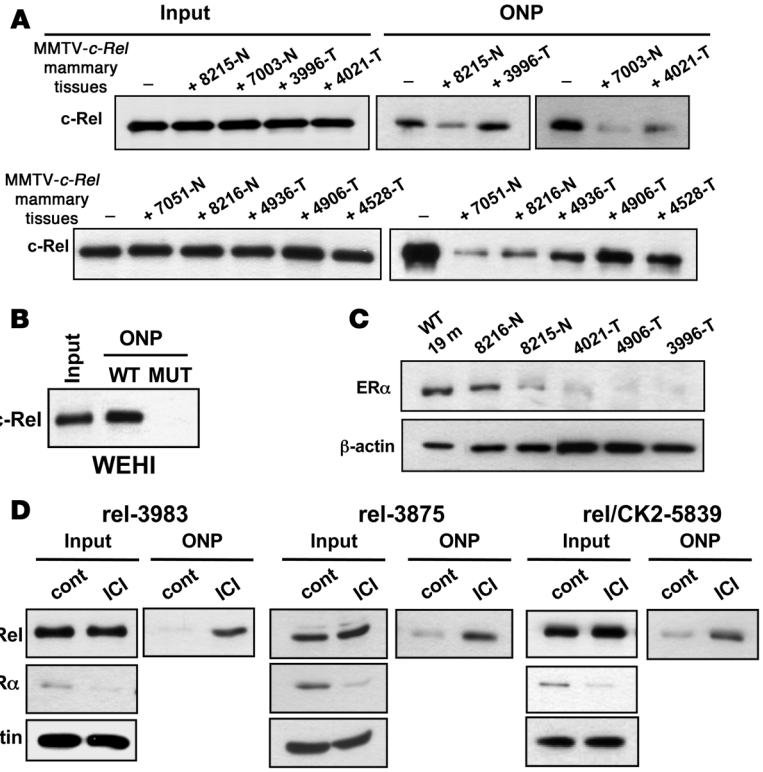

Figure 1
Inhibition of ERα signaling increases c-Rel DNA binding. (**A**) WCEs (250 μg) prepared from WEHI 231 cells were preincubated with WCEs (500 μg) prepared from the indicated MMTV–*c-Rel* mouse mammary tumor (T) (19-month-old mice) or histologically normal tissue (N) (2-month-old mice) or equivalent volume of lysis buffer (–) for a total of 100 μl. Samples (4 μl) were removed for analysis of input and the remaining WCE mixtures were subjected to ONP assay using an NF-κB element-containing oligonucleotide as probe and assessed for precipitated c-Rel protein (ONP). (**B**) WEHI 231 WCEs (250 μg) were subjected to ONP assay using an oligonucleotide containing either a wild-type or mutant (MUT) NF-κB element. Input: 15 μg WCEs was used. (**C**) WCEs (25 μg), prepared from the indicated MMTV–*c-Rel* mouse mammary tumor or histologically normal tissue or wild-type FVB/N 19-month-old mice were subjected to immunoblotting for ERα and β-actin, which confirmed equal loading of mammary tissue and tumor extracts. (**D**) rel-3983, rel-3875, and rel/CK2-5839 cells growing in low-serum medium were treated with 1 μM ICI 182,780 (ICI) or vehicle ethanol (Cont) for 48 hours. WCEs (500 μg) were then subjected to ONP assay, as in **A**. WCEs (15 μg) were used as input and subjected to immunoblotting for c-Rel, ERα, and β-actin, which confirmed equal loading.

(14). Recently, PKCθ has been shown to play an essential role in T cell and B cell activation by inducing NF-κB activity mainly via IκB kinase (IKKβ) (15, 16). An inverse relationship between ERα expression and the activity and levels of the conventional PKCα isoform was seen in breast cancer cell lines (17). These findings led us to hypothesize a role for PKC in the induction of mammary tumorigenesis by c-Rel. We identify, for what we believe is the first time, the novel PKCθ isoform as a critical regulator of c-Rel–driven mammary tumorigenesis. We confirm that ERα inhibits c-Rel DNA binding and transactivation in the mammary gland. PKCθ is elevated in transgenic mouse mammary tumors and in ERα-negative human breast cancers. PKCθ activates Akt, leading to decreased functional forkhead box O protein 3a (FOXO3a) and synthesis of its target genes *ER*α and $p27^{Kip1}$. The resulting derepression of c-Rel activity that allows for activation of critical targets, in combination with the decrease in $p27^{Kip1}$ synthesis, promotes proliferation and transformed phenotype of breast cancer cells. Derepression of c-Rel has potential clinical ramifications as breast cancer incidence in women increases during menopause, when E2/ERα signaling decreases (18).

Results

Identification of ERα as a potent inhibitor of c-Rel activity in mammary gland tissue. To determine whether a factor present in the mammary gland can inhibit c-Rel DNA binding, we used WEHI 231 B lymphomas whole cell extracts (WCEs), which are rich in highly functional p50/c-Rel complexes (19), and an oligonucleotide containing the NF-κB element upstream of the c-*myc* promoter in oligonucleotide precipitation (ONP) assays. Before addition of the oligonucleotide, WEHI 231 WCEs were preincubated with extracts prepared from histologically normal mammary glands or mammary tumors from MMTV–*c-Rel* mice. Similar levels of c-Rel were detected in extracts of the mammary tumors and normal tissues, and these were significantly lower than levels in the WCEs from WEHI 231 cells (ref. 5 and data not shown). All input c-Rel levels were essentially equivalent (Figure 1A). Immunoblot analysis for precipitated c-Rel showed that the normal mammary gland extracts profoundly inhibited c-Rel DNA binding in the WCE mixtures, whereas the presence of extracts from mammary tumors caused only a modest inhibition (Figure 1A). As a negative control, ONP analysis was performed using WEHI 231 WCEs and an oligonucleotide containing a mutant NF-κB element with 2 G-to-C residue transversions, which block NF-κB binding (20). Precipitated c-Rel protein was not detected by immunoblotting with the mutant oligonucleotide (Figure 1B), confirming the specificity of the binding.

Since ERα represses NF-κB activity (10, 21) and ERα protein levels were higher in normal mammary gland compared with mammary tumor extracts (Figure 1C), we hypothesized that ERα could be the inhibitory factor. To begin to assess the role of ERα signaling on c-Rel binding, cell lines derived from individual mammary tumors in MMTV–c-*Rel* and MMTV–c-*Rel*x*CK2*α transgenic mice were used. Cells were treated for 48 hours with the anti-estrogen ICI 182,780, which inhibits estrogen-dependent ERα function (22) and decreases ERα protein levels (23), and WCEs subjected to ONP analysis using the wild-type NF-κB oligonucleotide. ICI 182,780 treatment, which led to the expected decrease in ERα expression, strongly induced c-Rel DNA binding (Figure 1D). Moreover, ICI 182,780 treatment of rel-3875 cells caused an approximately 50% induction in NF-κB element–driven luciferase activity (39,674 ± 4,052 versus 75,046 ± 3,703; $P = 0.002$ by Student's *t* test). To further explore the effects of ERα signal-

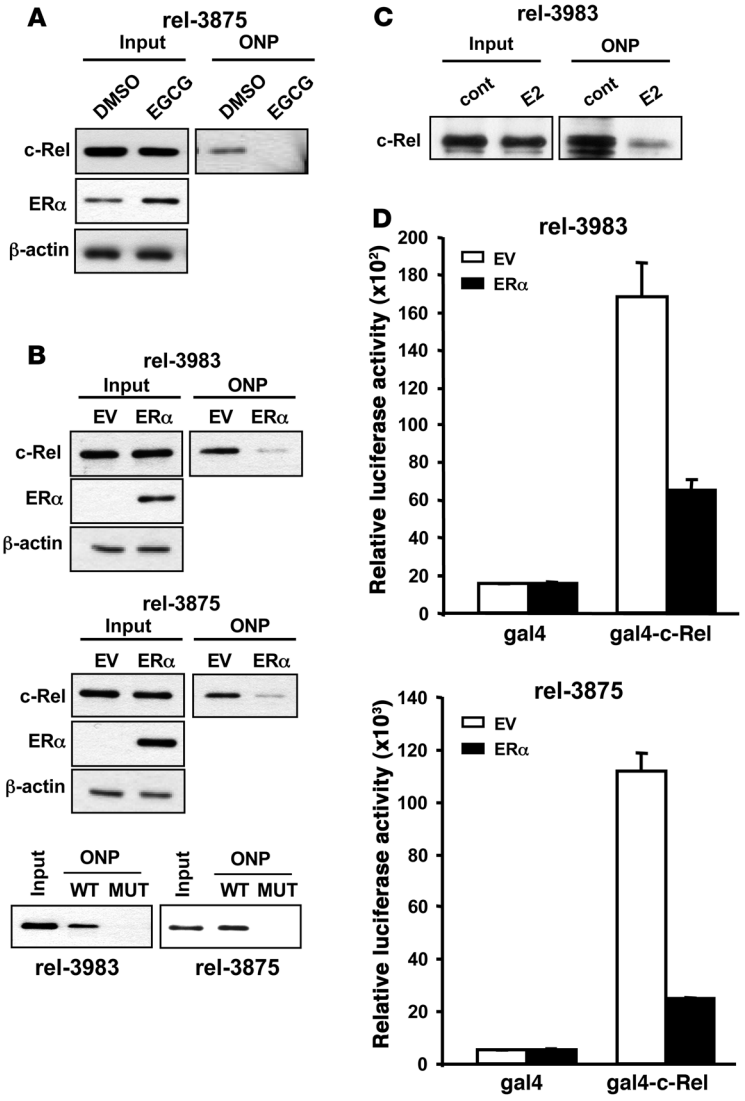

Figure 2
ERα represses c-Rel DNA binding and transactivation. (**A**) rel-3875 cells were treated for 48 hours with 60 μg/ml EGCG or vehicle DMSO. WCEs (500 μg) were then subjected to ONP assay as described in Figure 1D. Input: 15 μg WCEs were used. (**B**) rel-3983 and rel-3875 cells were transiently transfected with 6 μg ERα expression vector or EV, and 48 hours later WCEs (500 μg) were prepared and subjected to ONP assay, as described in Figure 1D. rel-3983 and rel-3875 WCEs (500 μg) were then subjected to ONP assay using an oligonucleotide containing either a wild-type or mutant NF-κB element. (**C**) rel-3983 cells in steroid-free medium were treated with 10 nM E2 or vehicle ethanol for 48 hours. WCEs (500 μg) were then subjected to ONP assay as described in Figure 1D. (**D**) rel-3983 and rel-3875 cells were transiently transfected in triplicate with 0.05 μg pG5E1B-Luc vector, β-gal, and 0.1 μg Gal4 or Gal4–c-Rel vectors and 0.1 μg ERα expression vector or EV, as indicated. The values represent the mean ± SD of luciferase activities normalized for β-gal activity.

ing on c-Rel activity, rel-3875 cells were treated with the green tea polyphenol epigallocatechin-3-gallate (EGCG), which induces ERα expression (24) (Figure 2A). EGCG treatment inhibited c-Rel DNA binding (Figure 2A). Importantly, ectopic expression of ERα in rel-3983 and rel-3875 cells very robustly repressed c-Rel binding (Figure 2B). As above, the specificity of the binding of c-Rel in the rel-3983 and rel-3875 WCEs was confirmed using the mutant NF-κB element in the ONP analysis (Figure 2B). Taken together, these results identify ERα as an inhibitor of c-Rel binding in mammary tumor cells.

To test whether this inhibition was ligand dependent, rel-3983 cells in medium depleted of steroids were incubated in the presence of E2 for 48 hours. ONP analysis showed that binding of c-Rel decreased after estradiol treatment (Figure 2C). We next assessed whether ERα could alter the transactivation properties of c-Rel using a mammalian 1-hybrid system. As expected, transfection of an expression plasmid coding for full-length mouse c-Rel fused to the Gal4 DNA-binding domain, and a Gal4-responsive promoter in rel-3983 and rel-3875 cells resulted in the induction of Gal4-driven luciferase activity compared with the basal luciferase activity detected with Gal4 (Figure 2D). Ectopic expression of ERα led to reduction in the transactivation ability of c-Rel. These data indicate that ERα represses both DNA binding and transactivation by c-Rel in mammary tumor cell lines.

Total PKC activity is elevated in MMTV–c-Rel mammary tumors. Given that PKC can regulate NF-κB activity (25, 26), we next compared PKC activity in mammary tumors and rel-3983 cells with histologically normal tissues from MMTV–*c-Rel* mice. WCEs immunoprecipitated with a pan-PKC antibody were tested in a kinase assay with exogenous histone H1 as substrate (27). All tumor samples and the cell line exhibited substantially elevated PKC activity compared with normal tissues, with the exception of 4936-T (Figure 3A). Negative controls of incubation with staurosporine, the potent pharmacological inhibitor of PKCs, and immunoprecipitation using normal rabbit IgG, confirmed the specificity of the assay for PKC. Immunoblot analysis of PKC expression showed that tumors 4906, 3996, 4556, and 4521 and rel-3983 cells expressed a higher level of PKC than normal tissues (Figure 3A). Tumors 4021, 3814, and 4528, which exhibited high PKC activity, displayed levels of PKC expression comparable with those seen in normal tissues. Thus PKC activity is higher in mouse mammary tumors and the derived cell line than in normal tissue.

c-Rel–driven mammary tumors and cell lines display elevated PKCθ activity. To determine whether PKC regulates the transcriptional activity of c-Rel, rel-3983 and rel/CK2-5839 cells were treated with staurosporine and WCEs subjected to ONP assay. Staurosporine inhibited c-Rel DNA interaction in both lines (Figure 3B). To further characterize the PKC isoform implicated in the regulation of c-Rel activity, the effects of more specific PKC inhibitors on c-Rel DNA binding were tested. Rottlerin, an inhibitor specific for PKCθ and PKCδ, caused a large inhibition in c-Rel DNA binding in rel-3983 and rel/CK2-5839 cells (Figure 3B), whereas Gö6983, which inhibits several PKCs including PKCδ but not PKCθ, had only a modest effect (Figure 3B), identifying PKCθ activation in the mammary tumor cell lines.

To test directly whether PKCθ was activated in c-Rel–induced mammary tumors, in vitro kinase assays were performed using an

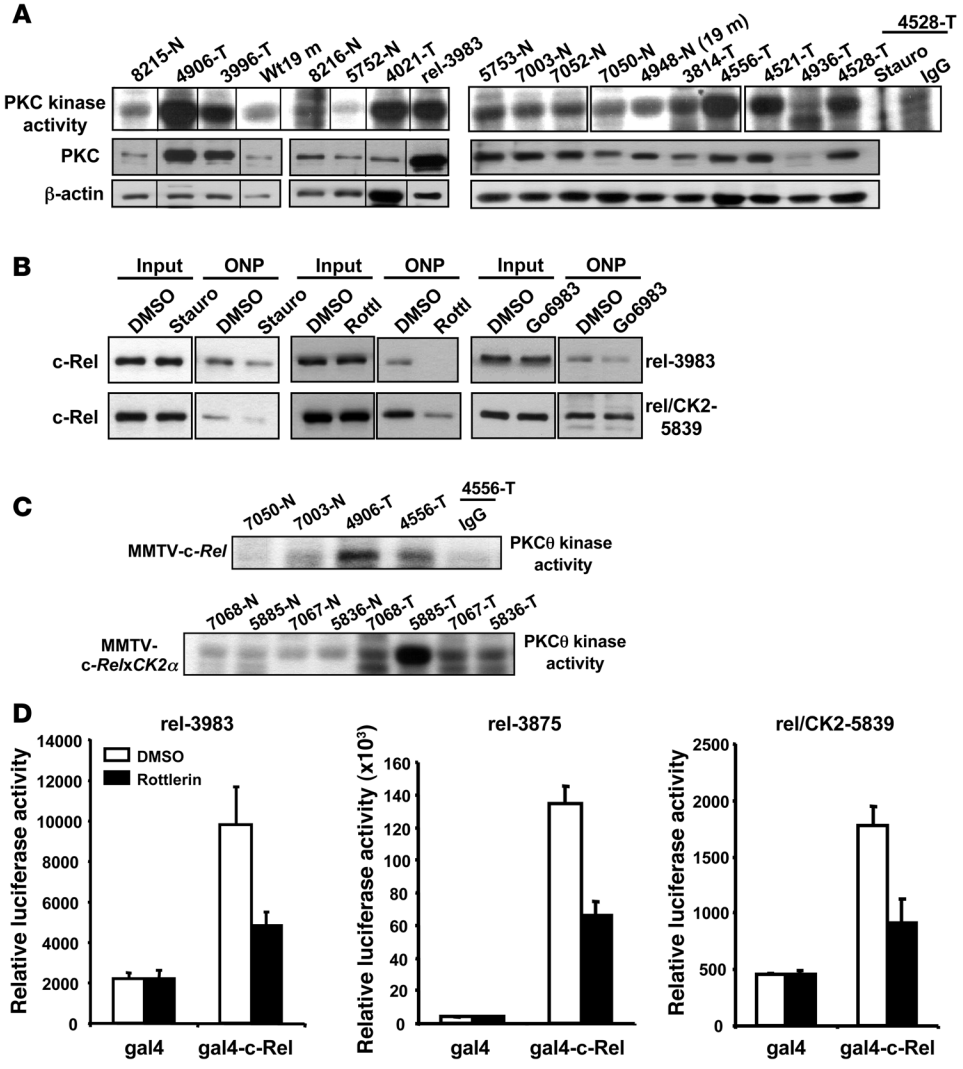

Figure 3

Inhibition of PKCθ with rottlerin reduces binding and transactivation by c-Rel. (**A**) WCEs (500 μg) prepared from MMTV–*c-Rel* mouse mammary tumors (19-month-old mice) and normal tissues (2-month-old mice, except 4948-N 19-month-old mice), were subjected to a PKC kinase assay (top). As controls for PKC kinase specificity, WCE from 4528-T was incubated with either normal IgG and the kinase reaction performed as described above or with PKC antibody, and the kinase reaction was performed in the presence of 25 nM staurosporine. Top: Samples were resolved on 1 gel (left panel) and on 2 gels (3 right panels). The 2 far-right panels were from 1 gel; these panels have been merged with the second gel to compare tumor and normal samples. Lanes were cut to align the sample order. Middle and bottom: WCEs used for the PKC kinase assay were run on 3 gels and subjected to immunoblotting for PKC and β-actin. Lanes were cut to align the sample order. WCEs from mammary glands of control wild-type FVB mice or transgenic animals (4948-N) (at 19 months of age) were similarly processed. (**B**) rel-3983 and rel/CK2-5839 cells were treated with 25 nM staurosporine (left), 5 μM rottlerin (middle), 1 μM Gö6983 (right), or DMSO for 20 hours, and WCEs (500 μg) were subjected to ONP assay, as described in Figure 1D. The input and the oligonucleotide precipitated proteins were run on the same gel but were noncontiguous. (**C**) WCEs (250 μg) prepared from the indicated mouse mammary tumor or normal tissue were subjected to a PKCθ kinase assay (62). As a negative control, WCE from 4556-T was incubated with normal IgG and similarly processed. (**D**) rel-3983, rel-3875, and rel/CK2-5839 cells were transiently transfected in triplicate with 0.05 μg pG5E1B-Luc vector, β-gal, or 0.1 μg Gal4 or Gal4–c-Rel vectors as indicated. Sixteen hours later, cells were treated with 5 μM rottlerin or DMSO for 20 hours and processed as described in Figure 2D.

antibody specific for PKCθ and WCEs from normal mouse mammary glands and mammary tumors. MMTV–*c-Rel* and MMTV–*c-RelxCK2*α tumors, but not normal mammary glands, exhibited a significant activation of PKCθ (Figure 3C). In contrast, only levels of PKCθ activity comparable with those obtained using normal rabbit IgG were detected in normal mammary tissues. Thus PKCθ activation occurs in c-Rel–induced mammary tumors.

*PKC*θ *positively regulates c-Rel transcriptional activity*. To begin to test the role of PKCθ in regulation of c-Rel activity, the effects of rottlerin treatment of rel-3983, rel-3875, and rel/CK2-5839 cells on the mammalian 1-hybrid system were monitored. Rottlerin led to a potent reduction of c-Rel transactivating ability (Figure 3D; rel-3983, $P = 0.016$; rel-3875, $P = 0.005$; rel/CK2-5839, $P = 0.028$ by Student's t test). In contrast, addition of Gö6983 had no significant effect on relative Gal4-driven luciferase activity (rel-3983, 13,985 ± 3,390 versus 16,617 ± 2,074; rel-3875: 134,686 ± 10,616 versus 113,164 ± 11,422 mean ± SD). To test directly the role of PKCθ in the regulation of c-Rel–mediated binding and transactivation ability, a commonly used kinase-defective PKCθ (PKCθ-K/R), which serves as a dominant negative for PKCθ activity, was employed (28). Inhibition of PKCθ activity in rel-3875 cells significantly reduced the binding of c-Rel (Figure 4A) and caused a dose-dependent decrease in the intrinsic c-Rel transactivation activity (Figure 4B). PKCθ-K/R expression also resulted in an approximately 2-fold reduction in NF-κB activity (Figure 4B). Similarly, expression of the PKCθ-K/R in the rel-3983 line inhibited NF-κB activity (Figure 4C) and transactivation by c-Rel (59,049 ± 7,695 versus 37,612 ± 1,434 where values represent the mean ± SD of relative Gal4-driven luciferase activity).

We next used constitutively active PKCθ (PKCθ-A/E) to test the effects of ectopic PKCθ expression on c-Rel–mediated activity. Expression of PKCθ-A/E in rel-3875 cells led to a potent induction of c-Rel transactivation (Figure 4D) and resulted in a greater than 5-fold increase in NF-κB activity (Figure 4D). Human breast cancer MCF7 cells, which express a high level of ERα, display very low levels of NF-κB binding and activity (21) and low total PKC activity (ref. 17 and see

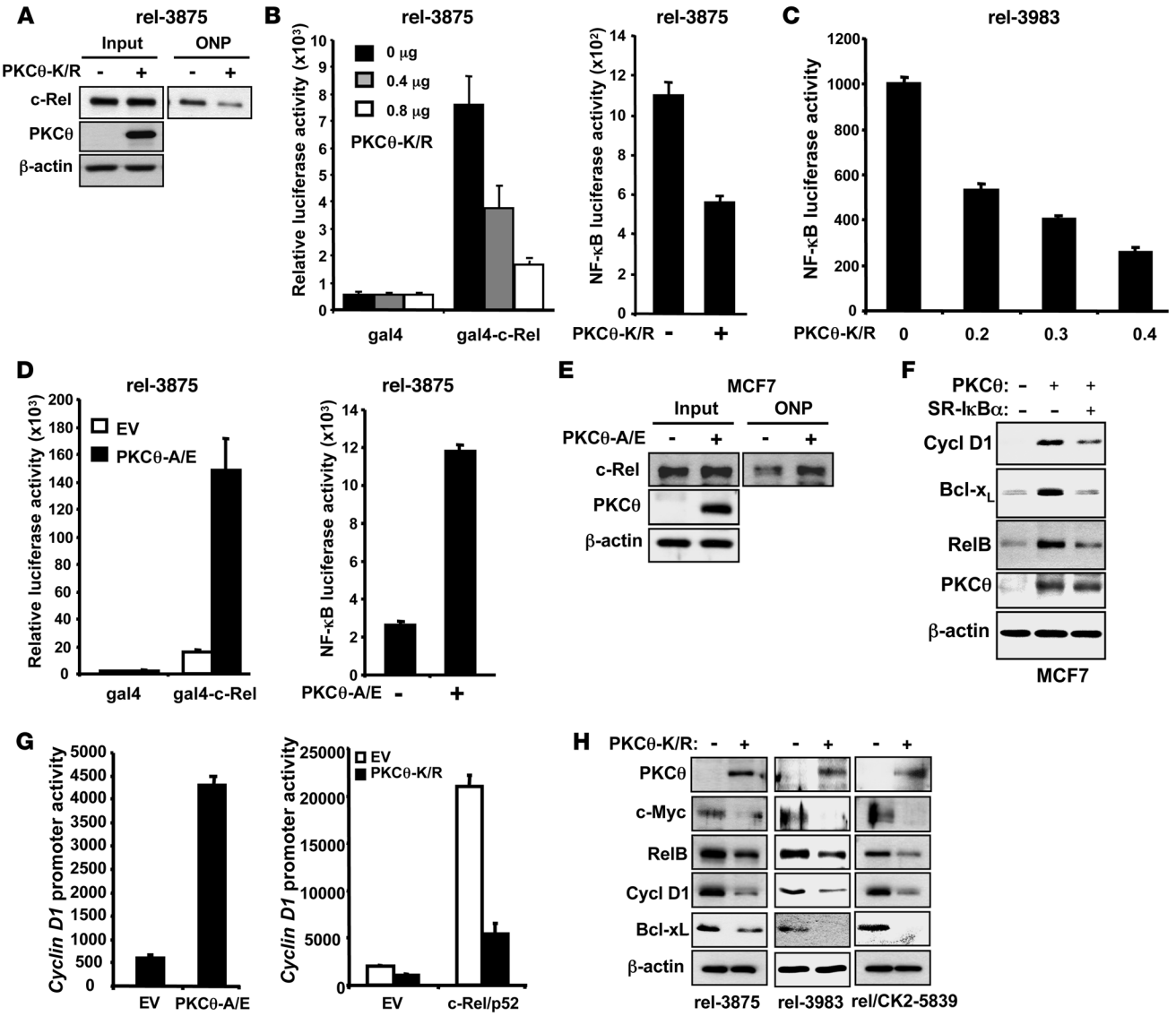

Figure 4

PKCθ regulates c-Rel transcriptional activity and target gene expression. (**A**) WCEs (500 μg) from rel-3875 cells transfected with 6 μg PKCθ-K/R or EV were subjected to ONP assay as described in Figure 1D. (**B**) Left: rel-3875 cells were transfected with 0.025 μg pG5E1B-Luc, β-gal, or 0.01 μg Gal4 or Gal4–c-Rel, along with 0.4 or 0.8 μg PKCθ-K/R or EV, and processed as described in Figure 2D. Right panel, rel-3875 cells were transfected with 0.1 μg NF-κB–Luc, β-gal, and 0.2 μg PKCθ-K/R or EV. Values represent the mean (± SD) of normalized luciferase activities. (**C**) rel-3983 cells were transfected with 0.1 μg NF-κB–Luc, β-gal, and 0.2, 0.3, or 0.4 μg PKCθ-K/R or EV and processed as above. (**D**) rel-3875 cells were transfected with 0.05 μg pG5E1B-Luc, β-gal, 0.1 μg Gal4 or Gal4–c-Rel, and 0.2 μg PKCθ-A/E or EV (left panel) or with 0.1 μg NF-κB–Luc, β-gal, and 0.2 μg PKCθ-A/E or EV (right panel) and processed as above. (**E**) WCEs (1,000 μg) from MCF7 cells transfected with 6 μg PKCθ-A/E or EV were subjected to ONP assay. Input: 15 μg WCEs. (**F**) WCEs from MCF7 cells transfected with 1 μg PKCθ-A/E or EV plus 2 μg SR-IκBα or EV were subjected to immunoblotting. (**G**) rel-3875 cells were transfected with 0.1 μg *cyclin D1* promoter driven–66-CD1-Luc and SV-40 β-gal in the presence of 0.2 μg PKCθ-A/E or EV (left panel) or 0.4 μg PKCθ-K/R or EV with either 0.2 μg c-Rel plus 0.2 μg p52 or EV (right panel). (**H**) WCEs from the indicated stable transfectants were subjected to immunoblotting.

Figure 5A). To determine whether ectopic PKCθ can induce c-Rel binding, MCF7 cells were transfected with the vector expressing the PKCθ-A/E. The resulting ONP analysis showed that PKCθ-A/E expression substantially enhanced c-Rel binding to the NF-κB site (Figure 4E). Taken together, these results demonstrate that PKCθ plays a critical role in the control of c-Rel transcriptional activity in *c-Rel*–driven mouse mammary tumors and human ERα-positive breast cancer cells.

PKCθ regulates endogenous c-Rel target gene expression and cyclin D1 promoter activity in breast cancer cells. Since PKCθ increases c-Rel activity, we next tested the effect of this protein kinase on the expression of products of 3 known target genes, cyclin D1, Bcl-x_L (5), and RelB (29). Expression of the PKCθ-A/E in MCF7 cells dramatically increased the endogenous levels of these 3 genes (Figure 4F). Coexpression of the IκBα inhibitory protein resulted in a partial or complete inhibition of this induction (Figure 4F), consistent with

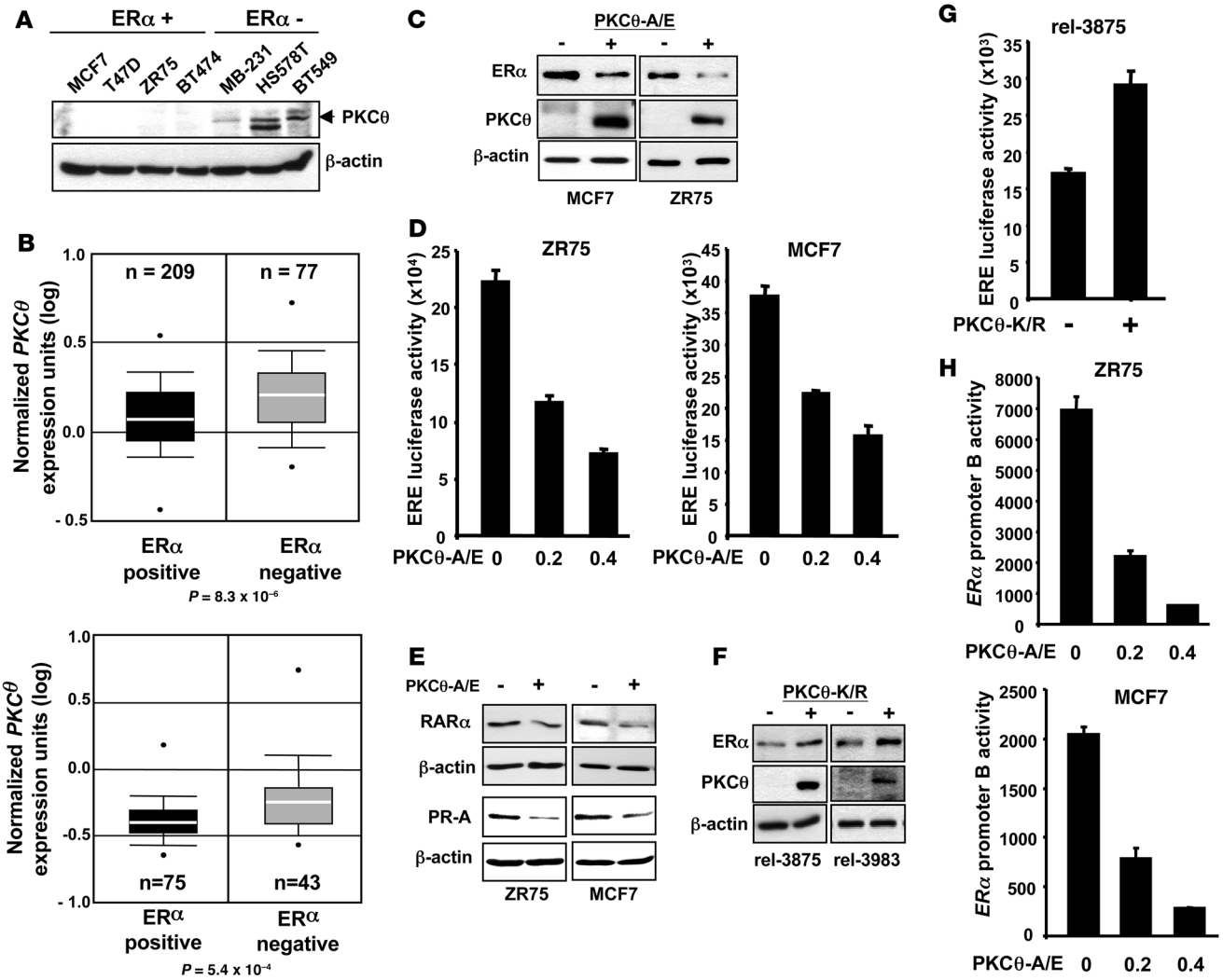

Figure 5

PKCθ inhibits ERα expression and activity. (**A**) WCEs from ERα-positive and ERα-negative human breast cancer cell lines were subjected to immunoblotting for PKCθ, position as indicated. (**B**) Box plots of data from the Wang et al. (30) (top panel) and Chin et al. (31) (bottom panel) carcinoma microarray datasets (reporter number 210039_s_at) were accessed using the ONCOMINE Cancer Profiling Database and were plotted on a log scale. A Student's *t* test performed directly through the Oncomine 3.0 software showed the difference in *PKC*θ expression between the 2 groups was significant (Wang et al. [ref. 30] dataset: $P = 8.3 \times 10^{-6}$ and Chin et al. [ref. 31] dataset: $P = 5.4 \times 10^{-4}$). (**C**) MCF7 and ZR75 cells were transfected in 6-well plates with 2 μg PKCθ-A/E or EV. WCEs were subjected to immunoblotting. (**D**) ZR75 and MCF7 cells were transfected in 12-well plates with 0.1 μg ERE2-tk-Luc, β-gal, and 0.2 or 0.4 μg PKCθ-A/E or EV. The values represent the mean ± SD of normalized luciferase activities. (**E**) WCEs from **C** were subjected to immunoblotting for RARα, PR-A, and β-actin. (**F**) rel-3875 and rel-3983 cells were transfected in 6-well plates with 2 μg PKCθ-K/R or EV. WCEs were subjected to immunoblotting. (**G**) rel-3875 cells were transfected in 12-well plates with 0.1 μg ERE-Luc, β-gal, and 0.4 μg PKCθ-K/R (+) or EV (–). (**H**) ZR75 and MCF7 cells were transfected in 12-well plates with 0.1 μg proB-Luc, β-gal, and 0.2 or 0.4 μg PKCθ-A/E or EV. The values represent the mean ± SD of normalized luciferase activities.

PKCθ-mediating stimulation of these genes via c-Rel NF-κB activity. Furthermore, expression of PKCθ-A/E in rel-3875 cells potently activated the *cyclin D1* promoter activity compared with control empty vector (EV) DNA (Figure 4G). The potent induction of *cyclin D1* promoter activity mediated by ectopic expression of c-Rel and p52 (Figure 4G), as seen previously (5), was repressed by approximately 75% upon expression of PKCθ-K/R (Figure 4G). Thus PKCθ regulates *cyclin D1* promoter activity driven by c-Rel.

The effects of the dominant-negative PKCθ on endogenous expression of c-Rel target genes in c-Rel–driven cell lines were next examined. Stable rel-3983, rel-3875, and rel/CK2-5839 cell populations with either the PKCθ-K/R or control EV DNA were analyzed by immunoblot analysis (Figure 4H). Ectopic expression of PKCθ-K/R led to significant decreases in c-Myc, RelB, cyclin D1, and Bcl-x_L protein levels (Figure 4H). Thus PKCθ is critical for maintenance of c-Rel target gene expression in MMTV–c-*Rel* and MMTV–c-*RelxCK2*α cell lines.

*Expression of ER*α *and PKC*θ *correlate inversely in human breast cancer tissues and cell lines.* To test whether PKCθ levels are higher in ERα-negative or -positive breast cancer cells, we subjected WCEs from 4 ERα-positive (MCF7, T47D, ZR75, and BT474), and 3 ERα-negative (MDA-MB-231, Hs578T, and BT549) human

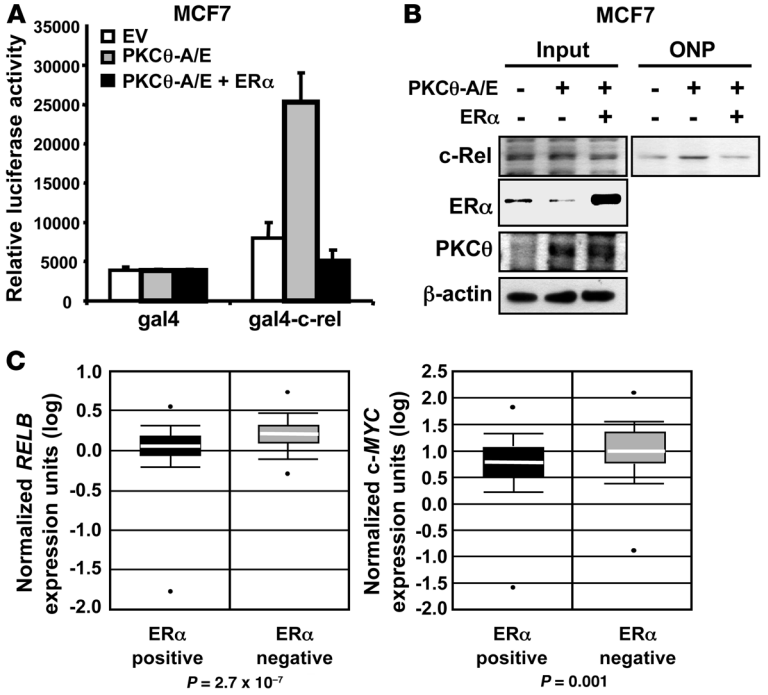

Figure 6
ERα overexpression blocks the stimulatory effect of PKCθ on c-Rel activity. (**A**) MCF7 cells were transiently transfected in triplicate with 0.05 μg pG5E1B-Luc vector, β-gal, 0.1 μg Gal4 or Gal4–c-Rel vectors, and 0.2 μg PKCθ-A/E either alone or in the presence of 0.1 μg ERα, or EV DNA and processed as described in Figure 2D. (**B**) MCF7 cells in P100 plates were transiently transfected with 4 μg PKCθ-A/E either alone or plus 2 μg ERα, or with EV as indicated, and 48 hours later WCEs (1,000 μg) were subjected to ONP assay as described in Figure 1D. The extent of decrease in ERα levels compared with those shown in Figure 5B is consistent with the lower amount of PKCθ expression. (**C**) The Wang et al. (30) carcinoma microarray dataset was analyzed for expression of *RELB* ($P = 2.7 \times 10^{-7}$) and c-*MYC* ($P = 0.001$) as described in Figure 5B.

breast cancer cell lines to immunoblotting for PKCθ. All 3 ERα-negative cell lines displayed more abundant levels of PKCθ compared with the 4 ERα-positive cell lines (Figure 5A). To extend our studies to primary human breast cancers, 2 microarray gene expression datasets using 286 (30) and 118 patients (31), publicly available at http://www.oncomine.org/geneModule/differential/filterStoreSummary.jsp?a=Analysis%20Type&b=Misc&c=Tissue&d=Breast&e=3, were analyzed. The levels of *PKC*θ mRNA were substantially higher in ERα-negative compared with ERα-positive breast cancers (Figure 5B). Statistical analysis of these breast cancer specimen datasets showed a significant inverse correlation between *ER*α and *PKC*θ mRNA ($P = 8.3 \times 10^{-6}$ for Wang et al. [ref. 30] dataset and $P = 5.4 \times 10^{-4}$ for Chin et al. [ref. 31] dataset, by Student's *t* test). Thus, ERα and PKCθ expression correlate inversely in human breast cancer. This inverse correlation suggested the possibility that PKCθ regulates ERα expression, which we investigated next.

*PKC*θ *inhibits ER*α *expression in breast cancer cells*. Ectopic expression of a PKCθ-A/E in ERα-positive MCF7 and ZR75 lines caused a substantial decrease in ERα protein levels (Figure 5C). To verify that inhibition of ERα expression was accompanied by a reduction in ERα function, we measured the effects of PKCθ-A/E on a 2-copy ERE-driven luciferase reporter activity and on the endogenous expression of retinoic acid receptor α (RARα) (32) and progesterone receptor A (PR-A) (33), 2 products of known target genes of ERα signaling. An increasing concentration of PKCθ-A/E vector in ZR75 and MCF7 cells resulted in a dose-dependent inhibition of ERE activity (Figure 5D). Furthermore, ectopic PKCθ-A/E reduced endogenous levels of RARα and PR-A proteins (Figure 5E). Conversely, expression of the PKCθ-K/R in the ERα-low rel-3875 and rel-3983 cells led to an induction of ERα expression (Figure 5F). Furthermore, a 1.7-fold induction in ERE activity was seen upon inhibition of PKCθ activity in rel-3875 cells (Figure 5G). Transcription of the human *ER*α gene occurs from 2 different promoters, promoter A (proximal) and promoter B (distal). Since studies have shown that promoter B plays an essential role in the regulation of *ER*α gene expression in human breast cancer (reviewed in ref. 24), we next asked whether PKCθ repressed transcription of this promoter. A dose-dependent decrease in human *ER*α promoter B activity was observed in both ZR75 and MCF7 cells upon expression of PKCθ-A/E (Figure 5H).

Lastly, we assessed whether ERα is a critical effector of PKCθ-induced activation of c-Rel activity. The increase in c-Rel transactivation function induced by PKCθ-A/E was completely suppressed by ectopic expression of ERα in MCF7 cells (Figure 6A). Furthermore, ectopic expression of ERα was sufficient to reverse PKCθ-mediated induction of c-Rel binding activity (Figure 6B). Consistent with these observations, expression of the c-Rel target genes *RELB* and c-*MYC* from Wang et al. (30) dataset were significantly higher in the ERα-negative human breast cancer tissues with elevated *PKC*θ expression (see Figure 5B) compared with ERα-positive specimens (Figure 6C). Similarly, the ERα-negative human breast cancer tissues obtained from Chin et al. (31) dataset displayed higher levels of *RELB* mRNA compared with the ERα-positive ones ($P = 2.1 \times 10^{-5}$) (data not shown). Thus PKCθ represses ERα expression and function in breast cancer cells, and this appears to play a critical role in the observed stimulation of c-Rel transcriptional activity by PKCθ, suggesting it is the critical downstream mediator.

*PKC*θ *inhibits FOXO3a, the transcriptional activator of ER*α *promoter B*. Recently we showed that FOXO3a potently activates *ER*α gene transcription from promoter B via binding to 2 upstream forkhead elements (24). Thus we investigated whether inactivation of FOXO3a mediates the effects of PKCθ on ERα expression. The PKCθ-A/E in MCF7 and ZR75 cells led to a prominent decrease in functional nuclear levels of FOXO3a protein, a commensurate decrease in ERα levels (Figure 7A), and reduced activity of a 3 copy forkhead element–driven luciferase reporters (5-fold in MCF7,

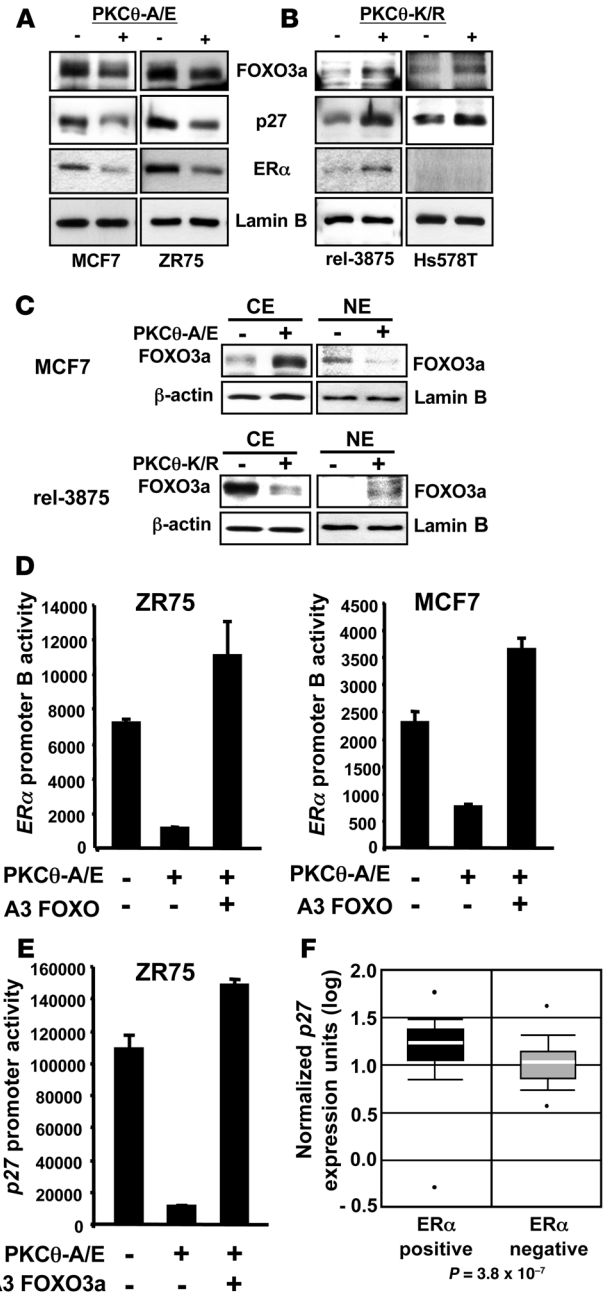

Figure 7
PKCθ inhibits functional FOXO3a protein level. (**A**) MCF7 and ZR75 cells were transiently transfected with 2 μg PKCθ-A/E (+) or EV (–) as indicated, and 48 hours later nuclear extracts were subjected to immunoblotting. (**B**) rel-3875 and Hs578T cells were transiently transfected with 2 μg PKCθ-K/R or EV as indicated, and 48 hours later nuclear extracts were subjected to immunoblotting, as in **A**. (**C**) Cytoplasmic extracts (CE) and nuclear extracts (NE) prepared from MCF7 cells transfected with 2 μg PKCθ-A/E or EV or from rel-3875 cells transfected with 2 μg PKCθ-K/R or EV were subjected to immunoblotting. (**D** and **E**) ZR75 and MCF7 cells were transiently transfected in triplicate with 0.1 μg of either proB-Luc vector (**D**) or *p27*-Luc vector (**E**) and β-gal, 0.2 μg PKCθ-A/E, or EV plus 0.05 μg A3 FOXO3a or EV DNA, as indicated. (**F**) The Wang et al. (30) carcinoma microarray dataset was analyzed for *p27* expression ($P = 3.8 \times 10^{-7}$), as described in Figure 5B.

155,343 ± 9,436 versus 33,233 ± 1,946; 9-fold in ZR75, 440,300 ± 7,137 versus 53,943 ± 9,674 mean ± SD of relative FHRE-driven luciferase activity), indicating reduced FOXO3a transcriptional activity. The cyclin-dependent kinase inhibitor (CKI) $p27^{Kip1}$ (*p27*) is another FOXO3a target gene. The endogenous nuclear levels of p27 protein were also decreased by expression of PKCθ-A/E (Figure 7A). Conversely, expression of PKCθ-K/R in rel-3875 cells resulted in a significant increase in functional FOXO3a expression as well as an induction of nuclear ERα and p27 protein levels (Figure 7B). The dominant-negative PKCθ similarly induced FOXO3a and p27 in the ERα-negative human Hs578T breast cancer cells, although in these cells the *ER*α promoter is silenced by hypermethylation (34), and was therefore not induced by this treatment (Figure 7B). FOXO3a cellular localization and activity is controlled by Akt phosphorylation, i.e., phospho-FOXO3a is bound by 14-3-3 and exported from the nucleus (35). We next investigated the effects of PKCθ on the cytoplasmic versus nuclear localization of FOXO3a. Expression of PKCθ-A/E in MCF7 led to an increase of FOXO3a in the cytoplasmic compartment while reducing its nuclear level (Figure 7C). Conversely, PKCθ-K/R expression in rel-3875 cells resulted in a decrease of FOXO3a in the cytoplasm and an increase in the nucleus (Figure 7C). To further test the role of FOXO3a as downstream mediator of PKCθ in the control of *ER*α gene transcription, the ability of a constitutively active form of FOXO3a, which cannot be phosphorylated by Akt, to reverse the effects of PKCθ were assessed (Figure 7D). Expression of a constitutively active A3 FOXO3a mutant in ZR75 and MCF7 cells completely blocked the repression of *ER*α promoter B activity induced by PKCθ. Similarly, PKCθ-A/E expression in ZR75 cells inhibited *p27* promoter activity, and this repression was reversed by the presence of A3 FOXO3a mutant (Figure 7E). Consistent with these findings, the ERα-negative human breast cancer tissues with high *PKC*θ expression (see Figure 5B) displayed lower levels of $p27^{Kip1}$ mRNA than ERα-positive tissues (Figure 7F). Thus PKCθ regulates *ER*α and $p27^{Kip1}$ transcription and protein levels through inhibition of functional FOXO3a.

*Activation of Akt by PKC*θ *inhibits FOXO3a.* Since Akt regulates the cellular localization and functional activity of FOXO3a (35), the ability of PKCθ to activate this kinase was next assessed. Expression of PKCθ-A/E in MCF7 and ZR75 cells resulted in a substantial increase in phosphorylated (Ser473) Akt, while no change was observed in total Akt protein level (Figure 8A). Conversely, expression of the PKCθ-K/R in rel-3875 cells significantly reduced phosphorylated Akt (Figure 8A). We next employed a kinase-defective Akt (Akt-DN), which acts as a dominant-negative for Akt activity, to determine whether PKCθ modulates the transcription of FOXO3a target genes via the Akt pathway. Expression of an increasing amount of Akt-DN in ZR75 cells reversed the inhibition of *ER*α and *p27* promoter activity by PKCθ in a dose-dependent manner (Figure 8B). In contrast, inhibition of IKKβ activity, which also negatively regulates the nuclear localization of FOXO3a (36), had no effect (data not shown). Thus PKCθ modulates transcription of FOXO3a target genes via activation of Akt.

Since Akt inhibits ERα expression through FOXO3a (24) and ERα represses c-Rel transcriptional activity, we next asked whether Akt can modulate c-Rel–mediated transformed phenotype, specifically proliferation and ability to migrate. For this purpose, stable populations of rel/CK2-5839 cells with EV DNA (control) or expressing a kinase-defective Akt (Akt-DN stable 1 and stable 2)

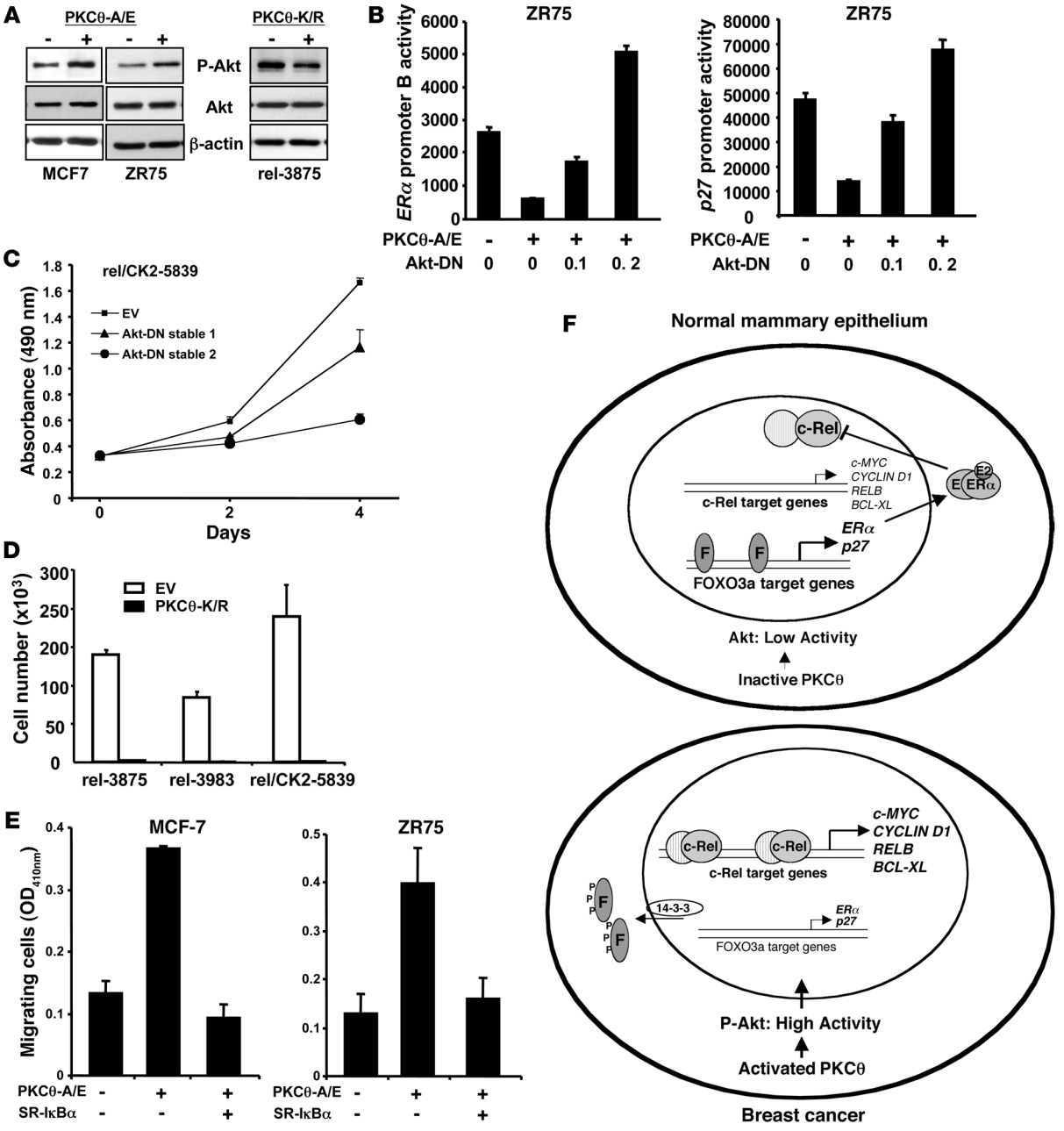

Figure 8

PKCθ activates Akt and promotes proliferation and migration of breast cancer cells. (**A**) WCEs from MCF7 and ZR75 cells transfected with 2 μg PKCθ-A/E or EV DNA (left panel) or rel-3875 cells transfected with 2 μg PKCθ-K/R or EV DNA were subjected to immunoblotting for phosphorylated Akt (p-Akt), total Akt, and β-actin. (**B**) ZR75 cells were transiently transfected in triplicate with 0.1 μg of proB-Luc vector (top panel) or *p27*-Luc vector (bottom panel) and β-gal, 0.2 μg PKCθ-A/E or EV DNA with either 0.1 or 0.2 μg Akt-DN or EV DNA. (**C** and **D**) The indicated cell lines stably expressing Akt-DN (**C**) or PKCθ-K/R (**D**) were subjected to either an MTS cell proliferation assay (**C**) or cell count (**D**). The values represent the mean ± SD. (**E**) MCF7 and ZR75 cells, transfected with 3 μg PKCθ-A/E or EV plus 6 μg SR-IκBα or EV, were subjected to a migration assay for 48 or 24 hours, respectively. Values represent mean ± SD of OD_{410nm}. (**F**) In the normal mammary gland, active FOXO3a leads to synthesis of ERα and $p27^{Kip1}$. ERα signaling inhibits c-Rel activity and expression of c-Rel target genes, and $p27^{Kip1}$ induces cell cycle arrest. Activation of PKCθ during mammary tumorigenesis induces activated Akt, leading to 14-3-3–mediated nuclear export of FOXO3a. The resulting inhibition of ERα synthesis causes derepression of c-Rel activity. Cell proliferation and migration are promoted via induction of expression of c-Rel target genes as well as by the decrease in $p27^{Kip1}$ synthesis.

were isolated (data not shown). Expression of the Akt-DN decreased the rate of proliferation, with the Akt-DN stable 2 population showing a more striking decline (Figure 8C). Furthermore, Akt-DN expression caused an approximately 3-fold reduction in migration of rel/CK2-5839 cells (0.22 ± 0.01 versus 0.07 ± 0.02 [stable 1] and versus 0.07 ± 0.01 [stable 2] mean OD_{410nm} ± SD)

compared with the control cells. Similarly, rel-3875 cells stably expressing the Akt-DN displayed inhibition of proliferation and migration (data not shown).

Given the roles of cyclin D1, c-Myc, and p27 in control of cell proliferation, we asked whether inhibition of PKCθ will reduce growth of MMTV–c-*Rel* and MMTV–c-*RelxCK2*α cell lines. Stable rel-3983, rel-3875, and rel/CK2-5839 cells with PKCθ-K/R expression or EV DNA were plated and cell numbers determined after incubation for 5 days (Figure 8D). Expression of PKCθ-K/R, detected in the cells (Figure 4H), potently inhibited cell proliferation, consistent with the modulation of target gene expression. These results were confirmed in the stable rel-3875 and rel-3983 cells using the nonradioactive MTS cell proliferation assay (data not shown). To further explore the role of PKCθ in c-Rel–driven tumorigenesis, the effect of PKCθ on migration of breast cancer cells was assessed. Ectopic expression of PKCθ-A/E potently increased the migration of MCF7 and ZR75 cells, and this induction was totally abolished by expression of IκBα, showing that these effects of PKCθ occur via c-Rel (Figure 8E).

Discussion

Here we show for what we believe to be the first time a critical role for PKCθ in mammary tumorigenesis by activation of Akt, which induced a pathway leading to derepression of c-Rel transcriptional activity (see model in Figure 8F). A critical mediator in this pathway is ERα signaling, which we observed repressed c-Rel binding and activity. Thus in normal breast epithelial cells, the activities of PKCθ and Akt were low, whereas that of FOXO3a was high (Figure 8F, upper panel). This led to ERα signaling, which repressed c-Rel, and induction of p27, which inhibits G1/S phase transition. Following activation of the PKCθ to Akt pathway, FOXO3a was phosphorylated and exported from the nucleus to the cytoplasm, where it is unable to activate the transcription of target genes *ER*α and *p27*. The resulting decrease in ERα protein derepressed c-Rel activity. The activation of c-Rel induced expression of genes encoding cyclin D1, c-Myc, and Bcl-x_L, which promote growth and survival, and RelB, which leads to a more invasive phenotype. Furthermore, the decrease in CKI $p27^{Kip1}$ protein levels alleviated the cell cycle arrest. Thus the induction of the PKCθ to Akt pathway promotes mammary tumorigenesis by inducing the full transactivation potential of c-Rel via inhibition of ERα signaling and by inactivating the growth inhibitory effects of FOXO3a. Consistent with this finding, we recently showed that constitutively active FOXO3a inhibits invasive phenotype of c-Rel–driven breast cancer cells (37). Interestingly, pregnancy levels of estrogen in rats have been shown to protect against mammary tumorigenesis induced by chemical carcinogens (38), which are known to induce NF-κB activity (2). The impact of repression of c-Rel by ERα signaling is particularly important, since high nuclear c-Rel levels were present in approximately 85% of human breast cancer samples (2). Of note, an inverse pattern of expression was seen between PKCθ and ERα in patient samples, and c-Rel target gene expression was higher in ERα-negative human breast cancer tissues. Consistently, statistical analysis of the Chin et al. (31) breast cancer specimen datasets showed a significant inverse correlation ($P = 3.2 \times 10^{-4}$) between mRNA levels of *PKC*θ and *PR*, a prototypical ERα target gene (data not shown). It is well known that breast cancer rates in women increase during menopause. Thus it is tempting to speculate that the release of repression of NF-κB activity by the drop in ERα signaling that occurs in menopause plays a critical role in breast disease in women.

Our findings showed that activation of Akt led to phosphorylation and inactivation of FOXO3a, and thereby to reduced *ER*α mRNA synthesis. Consistent with our findings, many groups have previously shown that Her-2/neu/Ras/Akt signaling reduces the levels of ERα (24, 39, 40). Thus it is interesting to note that Akt has also been found to enhance ERα activity (41, 42). ERα contains 2 activation domains, an aminoterminal AF-1 and a carboxyterminal AF-2 domain (9). While AF-2 requires hormone for activity, AF-1 is estrogen independent. Interestingly, Akt directly phosphorylates Ser167 within the AF-1 domain of ERα and enhances its activity several fold (41, 43). However, this appears to have little consequence for repression of NF-κB, which is hormone dependent and has been localized to the DNA binding and AF-2 domains of ERα (10). Thus the overall release of ERα-mediated repression of c-Rel by PKCθ in breast cancer cells can be attributed to a robust decline in hormone receptor levels or signaling.

Here we have identified a new mechanism of regulation of NF-κB activity by PKCθ via repression of the FOXO3a/ERα pathway. Induction of c-Rel DNA binding and transactivation by PKCθ appeared to occur mainly through inhibition of ERα signaling, since reexpression of ERα prevented this induction and ectopic FOXO3a expression similarly inhibited c-Rel transactivation (data not shown). ICI 182,780 treatment did not affect PKCθ protein levels or activity (data not shown), indicating the inverse regulation does not occur. The possibility that PKCθ controls NF-κB activity by other mechanisms in breast cancer cells cannot be excluded. In T cells, PKCθ stimulates NF-κB activity through IKKβ activation (15). IKKβ phosphorylates p65 and increases its transcriptional activity (44). IKKβ has recently been shown to phosphorylate the transactivation domain of c-Rel in vitro (45). Although the functional role of this phosphorylation has not been shown in vivo, the possibility that it similarly enhances functional c-Rel activity needs to be explored. A study found that PKCθ upregulated *c-Rel* gene transcription through NFAT in T cells (46). This regulation does not appear to occur in breast cancer cells, since PKCθ expression did not increase c-Rel protein levels in MCF7 or ZR75 cells. Moreover ERα-negative human breast cancer cell lines, which possessed elevated PKCθ activity, displayed similar c-Rel expression to ERα-positive lines but higher c-Rel DNA-binding (data not shown).

ERα-negative human breast cancer cell lines also express higher levels of PKCα compared with ERα-positive ones. PKCα has also been found to repress ERα protein levels and ERE-driven activity in T47D and in MCF7 (47, 48). Since PKCα activated PKCθ in T cells (49), the possibility exists that PKCα mediates inhibition of ERα expression via PKCθ signaling in breast cancer cells. While PKCθ activity was elevated in all MMTV–c-*Rel* and MMTV–*c-RelxCK2*α mammary tumors, this increase did not always correlate with an elevated level of PKCθ protein. One explanation for this observation could be differential accumulation of DAG with age in mammary tissue. Accumulation of DAG with age has been reported in liver and liver cell plasma membranes of rats (50). DAG is produced by sequential action of phospholipase D and phosphatidate phosphohydrolase, and the activities of both of these enzymes increased in the brain of aged rats (51). Furthermore, a high-fat diet increases total PKC activity but not protein levels in skin (52).

Studies have shown that the regulation by estrogens of cyclin D1 and c-Myc expression is crucial for the proliferation of ERα-positive breast tumor cells (53). Our findings suggest that strong expression of PKCθ could lead to estrogen-independent growth by stimulating expression of these estrogen target genes. In addi-

tion, PKCθ reduces active nuclear FOXO3a and thereby inhibits expression of p27, a CKI that promotes cell cycle arrest. Of note, many aggressive cancers are typified by decreased levels of p27 (54). Furthermore, inactive cytoplasmic FOXO3a expression correlated with poor survival in breast cancer patients (36), consistent with the analysis showing that the mRNA levels of its target *p27* were lower in the ERα-negative human breast cancers, with known poorer overall survival. In summary, our findings identify PKCθ as a critical regulator of c-Rel–driven mammary tumorigenesis.

Methods

Cell growth and treatment conditions. Creation of the transgenic MMTV–c-*Rel*, MMTV-*CK2α*, and MMTV-c-*RelxCK2α* mice was described previously (5, 7, 8). Mammary cell lines were derived from mammary tumors by explant. The rel-3983, rel-3875, and rel/CK2-5839 cell lines were derived from MMTV–c-*Rel* #3983 tumor (adenosquamous cell carcinoma), MMTV–c-*Rel* #3875 tumor (mammary adenocarcinoma with poorly differentiated large cells), and MMTV–c-*RelxCK2α* #5839 tumor (mammary adenocarcinoma), respectively. The human breast cancer cell lines were purchased from the ATCC and maintained in standard culture medium as recommended by ATCC. WEHI 231 immature B lymphoma cells were cultured as described previously (19). EGCG and ICI 182,780 were purchased from LKT Laboratories and Tocris Cookson, respectively. Estradiol, staurosporine, and puromycin were from Sigma-Aldrich. Rottlerin and Gö6983 were from Calbiochem, and zeocin was from Invitrogen.

Plasmid constructs and transfection analysis. The expression vectors Gal4 and Gal4–c-Rel were generously provided by Tom Gilmore (Boston University, Boston, Massachusetts, USA). The Gal4-inducible reporter pG5E1B-Luc was constructed as described in ref. 55. The NF-κB element–driven (NF-κB–Luc) and the *cyclin D1* promoter (–66CD1-Luc) constructs were constructed as previously reported (8). The SR-IκBα construct containing IκBα 32SS/36AA mutant in pRC–β-actin expression vector was constructed as previously reported (56). The PKCθ constitutively active (PKCθ-A/E) and PKCθ kinase-defective (PKCθ-K/R), subcloned in the pEF4/His expression vector, were generously provided by Amnon Altman (La Jolla Institute for Allergy and Immunology, San Diego, California, USA) (57). The human *ERα* promoter B in pGL3Basic (proB-Luc) was kindly provided by Shin-Ichi Hayashi (Saitama Cancer Center Research Institute, Saitama, Japan) (24). The pcDNA3-ERα expression vector and the reporter plasmid ERE2-tk-Luc were constructed as previously reported (58). In the constitutively active A3 FOXO3a mutant, the 3 sites of Akt phosphorylation (T32, S253, and S315) were mutated to alanine residues (35). The forkhead response element–luciferase (FHRE-luciferase) reporter gene containing 3 canonical FOXO binding sites was constructed as previously reported (59). The Akt and FHRE reporter vectors were kindly provided by Michael Greenberg and Anne Brunet (Harvard Medical School, Boston, Massachusetts, USA). The *p27* promoter luciferase reporter construct and Akt-DN expression vector were constructed as described in ref. 54 and ref. 60, respectively. To normalize transfection efficiency, 0.1 μg SV40 β-gal reporter vector (5) was used. For reporter assays, cells were transfected in triplicate in 12-well dishes with the amounts of DNA indicated in the figure legends using FuGene6 Transfection Reagent (Roche Diagnostics) 24 hours after plating. After 48 hours, luciferase assays were performed as previously described (5). For immunoblot and ONP assays, cells were plated in 6-well plates and p100 plates, respectively, and harvested 48 hours after transfection. Results obtained in immunoblot, ONP, and luciferase assays are representative of 3 separate experiments. To generate PKCθ-K/R stable transfectants, cells were transfected with 6 μg DNA in p100 plates and maintained in medium containing 1 mg/ml zeocin for 1 week. Akt-DN and control stable transfectants were generated by cotransfection of 5.5 μg of kinase-inactive K197M mutant Akt, which functions as Akt-DN (61) or EV DNA, with pGKpuro selection plasmid in p100 plates and selection with puromycin (4 μg/ml) for 2 weeks.

PKC kinase assay. WCEs from frozen tissue powders or cell pellets were immunoprecipitated with either a PKC or PKCθ antibody and then subjected to a kinase assay using histone H1 substrate, as previously described (27).

Immunoblot analysis and antibodies. WCEs (20 μg) and cytoplasmic (10 μg) and nuclear extracts (30 μg) were prepared and subjected to immunoblotting as previously described (24). Antibodies used were as follows: c-Rel (sc-71), RelB (sc-226), PKC (sc-10800), PKCθ (sc-212), ERα (sc-542; used only for analysis of tissue extracts), p27 (sc-776), and Bcl-x_L (sc-8392) (all from Santa Cruz Biotechnology Inc.); ERα (MS-1071; NeoMarkers); cyclin D1 (Ab-3; Oncogene); Akt and phospho-Akt (Ser473; Cell Signaling); FOXO3a (Upstate Biotechnology); RARα (Affinity Bioreagents); and β-actin (AC-15; Sigma-Aldrich). c-Myc and PR antibodies were kind gifts of Stephen Hann (Vanderbilt University, Nashville, Tennessee, USA) and Abdul Traish (Boston University School of Medicine, Boston, Massachusetts, USA), respectively.

Biotinylated ONP assay. Cells were rinsed with cold PBS and harvested in HKMG lysis buffer (10 mM HEPES, pH 7.9, 100 mM KCl, 5 mM $MgCl_2$, 10% glycerol, 0.5% NP-40) containing protease and phosphatase inhibitors. WCEs were obtained by sonication, and debris was removed by centrifugation. For ONP assays, samples (500 or 1,000 μg) were precleared with streptavidin-agarose beads, then incubated with 1 μg 5′-biotinylated double-stranded oligonucleotides and 5 μg poly(dI-dC) for 16 hours. DNA-bound proteins were collected with streptavidin-agarose beads and subjected to immunoblotting with c-Rel antibody. The sequence of the oligonucleotide containing the NF-κB element upstream of the c-*myc* promoter was 5′-AAGTCCGGGGTTTTCCCCAAC-3′, in which the underlining indicates the core element. The mutant NF-κB element, which has a double G-to-C transversion (denoted by bold font): 5′-AAGTCC**GCC**TTTTCCCCAAC-3′, displays greatly reduced NF-κB binding and activity (20).

Preparation of WCEs from mammary tissue. Frozen tissues from histologically normal mammary gland and breast tumors were pulverized in liquid nitrogen with a mortar and pestle. Frozen tissue powders were resuspended in HKMG or PKC lysis buffer (see above) and samples were Dounce homogenized for 20 strokes with a loose pestle and then 20 strokes with a tight pestle. WCEs were obtained by sonication and debris removed by centrifugation.

Gene expression and statistical analysis. The Wang et al. (30) carcinoma microarray dataset (reporter number 210039_s_at) and the Chin et al. (31) carcinoma microarray dataset (reporter number 210039_s_at) were accessed using the ONCOMINE Cancer Profiling Database (http://www.oncomine.org/geneModule/differential/filterStoreSummary.jsp?a=Analysis%20Type&b=Misc&c=Tissue&d=Breast&e=3). These datasets include 77 ERα-negative and 209 ERα-positive human primary breast carcinoma samples, and 43 ERα-negative and 75 ERα-positive human primary breast carcinoma samples, respectively. Box plots depicting the distribution of *PKCθ*, *RELB*, c-*MYC,* and *p27* expression within each ERα group, and a Student's *t* test giving a *P* value for the comparison of each gene expression between the 2 ERα groups, were obtained directly through the Oncomine 3.0 software. In Figures 5–7, the line within the boxes represent the median expression value for each group, and the upper and lower edges of the boxes indicate the 75th and 25th percentiles of the distribution, respectively. The lines (whiskers) emerging from each box extend to the smallest and largest observations; the black dots outside the ends of the whiskers are outlier data points.

Cell proliferation assay. For the nonradioactive MTS cell proliferation assay, stable transfectants expressing Akt-DN were plated in triplicate

at a density of 500 cells in 96-well plates. At the indicated time, the number of metabolically active cells was determined by conversion of MTS dye to its formazan product, read at A_{490nm} using the CellTiter 96 AQ assay kit (Promega) according to the manufacturer's direction. For the stable transfectants expressing PKCθ-K/R, cells were plated in triplicate at a density of 1×10^4 cells in 12-well plates. After 5 days, cell numbers were determined by counting. Results are representative of 2 separate assays.

Migration assay. Suspensions of 2×10^5 to 5×10^5 cells were layered in triplicate in the upper compartment of a Transwell (Costar) on an 8-mm-diameter polycarbonate filter (8-μm pore size) and incubated at 37°C for the indicated times. Migration of the cells to the lower side of the filter was evaluated with the acid phosphatase enzymatic assay using p-nitrophenyl phosphate and OD_{410nm} determination. Results are representative of 2 separate assays.

Acknowledgments

We thank Michael Greenberg, Anne Brunet, Amnon Altman, Tom Gilmore, Shin-Ichi Hayashi, Myles Brown, Steve Hann, and Abdul Traish for generously providing cloned DNAs, promoter constructs, and antibodies. This work was supported by grants from the National Institute of Environmental Health Sciences, the National Cancer Institute of the NIH, and the Avon Foundation.

Received for publication April 17, 2007, and accepted in revised form September 19, 2007.

Address correspondence to: Gail E. Sonenshein, Department of Biochemistry, Boston University School of Medicine, 715 Albany Street, Boston, Massachusetts 02118, USA. Phone: (617) 638-4120; Fax: (617) 638-4252; E-mail: gsonensh@bu.edu.

1. Ghosh, S., and Karin, M. 2002. Missing pieces in the NF-kappaB puzzle. *Cell.* **109**(Suppl.):S81–S96.
2. Sovak, M.A., et al. 1997. Aberrant nuclear factor-kappaB/Rel expression and the pathogenesis of breast cancer. *J. Clin. Invest.* **100**:2952–2960.
3. Rayet, B., and Gelinas, C. 1999. Aberrant rel/nfkb genes and activity in human cancer. *Oncogene.* **18**:6938–6947.
4. Cogswell, P.C., Guttridge, D.C., Funkhouser, W.K., and Baldwin, A.S., Jr. 2000. Selective activation of NF-kappa B subunits in human breast cancer: potential roles for NF-kappa B2/p52 and for Bcl-3. *Oncogene.* **19**:1123–1131.
5. Romieu-Mourez, R., et al. 2003. Mouse mammary tumor virus c-rel transgenic mice develop mammary tumors. *Mol. Cell. Biol.* **23**:5738–5754.
6. Romieu-Mourez, R., Landesman-Bollag, E., Seldin, D.C., and Sonenshein, G.E. 2002. Protein kinase CK2 promotes aberrant activation of nuclear factor-kappaB, transformed phenotype, and survival of breast cancer cells. *Cancer Res.* **62**:6770–6778.
7. Landesman-Bollag, E., et al. 2001. Protein kinase CK2 in mammary gland tumorigenesis. *Oncogene.* **20**:3247–3257.
8. Eddy, S.F., et al. 2005. Inducible IkappaB kinase/IkappaB kinase epsilon expression is induced by CK2 and promotes aberrant nuclear factor-kappaB activation in breast cancer cells. *Cancer Res.* **65**:11375–11383.
9. Matthews, J., and Gustafsson, J.A. 2003. Estrogen signaling: a subtle balance between ER alpha and ER beta. *Mol. Interv.* **3**:281–292.
10. Kalaitzidis, D., and Gilmore, T.D. 2005. Transcription factor cross-talk: the estrogen receptor and NF-kappaB. *Trends Endocrinol. Metab.* **16**:46–52.
11. Wang, X., et al. 2007. Oestrogen signalling inhibits invasive phenotype by repressing RelB and its target BCL2. *Nat. Cell Biol.* **9**:470–478.
12. O'Brian, C., Vogel, V.G., Singletary, S.E., and Ward, N.E. 1989. Elevated protein kinase C expression in human breast tumor biopsies relative to normal breast tissue. *Cancer Res.* **49**:3215–3217.
13. Gordge, P.C., Hulme, M.J., Clegg, R.A., and Miller, W.R. 1996. Elevation of protein kinase A and protein kinase C activities in malignant as compared with normal human breast tissue. *Eur. J. Cancer.* **32A**:2120–2126.
14. Newton, A.C. 1997. Regulation of protein kinase C. *Curr. Opin. Cell Biol.* **9**:161–167.
15. Lin, X., O'Mahony, A., Mu, Y., Geleziunas, R., and Greene, W.C. 2000. Protein kinase C-theta participates in NF-kappaB activation induced by CD3-CD28 costimulation through selective activation of IkappaB kinase beta. *Mol. Cell. Biol.* **20**:2933–2940.
16. Krappmann, D., Patke, A., Heissmeyer, V., and Scheidereit, C. 2001. B-cell receptor- and phorbol ester-induced NF-kappaB and c-Jun N-terminal kinase activation in B cells requires novel protein kinase C's. *Mol. Cell. Biol.* **21**:6640–6650.
17. Borner, C., Wyss, R., Regazzi, R., Eppenberger, U., and Fabbro, D. 1987. Immunological quantitation of phospholipid/Ca2+-dependent protein kinase of human mammary carcinoma cells: inverse relationship to estrogen receptors. *Int. J. Cancer.* **40**:344–348.
18. McPherson, K., Steel, C.M., and Dixon, J.M. 2000. ABC of breast diseases. Breast cancer-epidemiology, risk factors, and genetics. *BMJ.* **321**:624–628.
19. Lee, H., et al. 1995. Role of Rel-related factors in control of c-myc gene transcription in receptor-mediated apoptosis of the murine B cell WEHI 231 line. *J. Exp. Med.* **181**:1169–1177.
20. Duyao, M.P., Buckler, A.J., and Sonenshein, G.E. 1990. Interaction of an NF-kappa B-like factor with a site upstream of the c-myc promoter. *Proc. Natl. Acad. Sci. U. S. A.* **87**:4727–4731.
21. Nakshatri, H., Bhat-Nakshatri, P., Martin, D.A., Goulet, R.J., Jr., and Sledge, G.W., Jr. 1997. Constitutive activation of NF-kappaB during progression of breast cancer to hormone-independent growth. *Mol. Cell. Biol.* **17**:3629–3639.
22. Hyder, S.M., Chiappetta, C., Murthy, L., and Stancel, G.M. 1997. Selective inhibition of estrogen-regulated gene expression in vivo by the pure antiestrogen ICI 182,780. *Cancer Res.* **57**:2547–2549.
23. Oliveira, C.A., et al. 2003. The antiestrogen ICI 182,780 decreases the expression of estrogen receptor-alpha but has no effect on estrogen receptor-beta and androgen receptor in rat efferent ductules. *Reprod. Biol. Endocrinol.* **1**:75.
24. Guo, S., and Sonenshein, G.E. 2004. Forkhead box transcription factor FOXO3a regulates estrogen receptor alpha expression and is repressed by the Her-2/neu/phosphatidylinositol 3-kinase/Akt signaling pathway. *Mol. Cell. Biol.* **24**:8681–8690.
25. Isakov, N., and Altman, A. 2002. Protein kinase C(theta) in T cell activation. *Annu. Rev. Immunol.* **20**:761–794.
26. Moscat, J., Rennert, P., and Diaz-Meco, M.T. 2006. PKCzeta at the crossroad of NF-kappaB and Jak1/Stat6 signaling pathways. *Cell Death Differ.* **13**:702–711.
27. Chen, C.Y., and Faller, D.V. 1999. Selective inhibition of protein kinase C isozymes by Fas ligation. *J. Biol. Chem.* **274**:15320–15328.
28. Baier-Bitterlich, G., et al. 1996. Protein kinase C-theta isoenzyme selective stimulation of the transcription factor complex AP-1 in T lymphocytes. *Mol. Cell. Biol.* **16**:1842–1850.
29. Mineva, N.D., Rothstein, T.L., Meyers, J.A., Lerner, A., and Sonenshein, G.E. 2007. CD40 ligand-mediated activation of the de novo RelB NF-kappaB synthesis pathway in transformed B cells promotes rescue from apoptosis. *J. Biol. Chem.* **282**:17475–17485.
30. Wang, Y., et al. 2005. Gene-expression profiles to predict distant metastasis of lymph-node-negative primary breast cancer. *Lancet.* **365**:671–679.
31. Chin, K., et al. 2006. Genomic and transcriptional aberrations linked to breast cancer pathophysiologies. *Cancer Cell.* **10**:529–541.
32. Rishi, A.K., et al. 1995. Estradiol regulation of the human retinoic acid receptor alpha gene in human breast carcinoma cells is mediated via an imperfect half-palindromic estrogen response element and Sp1 motifs. *Cancer Res.* **55**:4999–5006.
33. Kastner, P., et al. 1990. Two distinct estrogen-regulated promoters generate transcripts encoding the two functionally different human progesterone receptor forms A and B. *EMBO J.* **9**:1603–1614.
34. Ottaviano, Y.L., et al. 1994. Methylation of the estrogen receptor gene CpG island marks loss of estrogen receptor expression in human breast cancer cells. *Cancer Res.* **54**:2552–2555.
35. Brunet, A., et al. 1999. Akt promotes cell survival by phosphorylating and inhibiting a Forkhead transcription factor. *Cell.* **96**:857–868.
36. Hu, M.C., et al. 2004. IkappaB kinase promotes tumorigenesis through inhibition of forkhead FOXO3a. *Cell.* **117**:225–237.
37. Belguise, K., Guo, S., and Sonenshein, G.E. 2007. Activation of FOXO3a by the green tea polyphenol epigallocatechin-3-gallate induces estrogen receptor alpha expression reversing invasive phenotype of breast cancer cells. *Cancer Res.* **67**:5763–5770.
38. Sivaraman, L., and Medina, D. 2002. Hormone-induced protection against breast cancer. *J. Mammary Gland Biol. Neoplasia.* **7**:77–92.
39. Stoica, A., Saceda, M., Doraiswamy, V.L., Coleman, C., and Martin, M.B. 2000. Regulation of estrogen receptor-alpha gene expression by epidermal growth factor. *J. Endocrinol.* **165**:371–378.
40. Clayton, S.J., May, F.E., and Westley, B.R. 1997. Insulin-like growth factors control the regulation of oestrogen and progesterone receptor expression by oestrogens. *Mol. Cell. Endocrinol.* **128**:57–68.
41. Campbell, R.A., et al. 2001. Phosphatidylinositol 3-kinase/AKT-mediated activation of estrogen receptor alpha: a new model for anti-estrogen resistance. *J. Biol. Chem.* **276**:9817–9824.
42. Martin, M.B., et al. 2000. A role for Akt in mediating the estrogenic functions of epidermal growth factor and insulin-like growth factor I. *Endocrinology.* **141**:4503–4511.
43. Sun, M., et al. 2001. Phosphatidylinositol-3-OH Kinase (PI3K)/AKT2, activated in breast cancer, regulates and is induced by estrogen receptor alpha (ERalpha) via interaction between ERalpha and PI3K. *Cancer Res.* **61**:5985–5991.
44. Yang, F., Tang, E., Guan, K., and Wang, C.Y. 2003. IKK beta plays an essential role in the phosphorylation of RelA/p65 on serine 536 induced by lipopolysaccharide. *J. Immunol.* **170**:5630–5635.
45. Harris, J., et al. 2006. Nuclear accumulation of cRel following C-terminal phosphorylation by TBK1/IKK epsilon. *J. Immunol.* **177**:2527–2535.

46. Grumont, R., et al. 2004. The mitogen-induced increase in T cell size involves PKC and NFAT activation of Rel/NF-kappaB-dependent c-myc expression. *Immunity.* **21**:19–30.
47. Ways, D.K., et al. 1995. MCF-7 breast cancer cells transfected with protein kinase C-alpha exhibit altered expression of other protein kinase C isoforms and display a more aggressive neoplastic phenotype. *J. Clin. Invest.* **95**:1906–1915.
48. Tonetti, D.A., Chisamore, M.J., Grdina, W., Schurz, H., and Jordan, V.C. 2000. Stable transfection of protein kinase C alpha cDNA in hormone-dependent breast cancer cell lines. *Br. J. Cancer.* **83**:782–791.
49. Trushin, S.A., et al. 2003. Protein kinase Calpha (PKCalpha) acts upstream of PKCtheta to activate IkappaB kinase and NF-kappaB in T lymphocytes. *Mol. Cell. Biol.* **23**:7068–7081.
50. Kavok, N.S., Krasilnikova, O.A., and Babenko, N.A. 2003. Increase in diacylglycerol production by liver and liver cell nuclei at old age. *Exp. Gerontol.* **38**:441–447.
51. Salvador, G.A., Pasquare, S.J., Ilincheta de Boschero, M.G., and Giusto, N.M. 2002. Differential modulation of phospholipase D and phosphatidate phosphohydrolase during aging in rat cerebral cortex synaptosomes. *Exp. Gerontol.* **37**:543–552.
52. Birt, D.F. 1995. Dietary modulation of epidermal protein kinase C: mediation by diacylglycerol. *J. Nutr.* **125**:1673S–1676S.
53. Doisneau-Sixou, S.F., et al. 2003. Estrogen and antiestrogen regulation of cell cycle progression in breast cancer cells. *Endocr. Relat. Cancer.* **10**:179–186.
54. Yang, W., et al. 2001. Repression of transcription of the p27(Kip1) cyclin-dependent kinase inhibitor gene by c-Myc. *Oncogene.* **20**:1688–1702.
55. Seth, A., Gonzalez, F.A., Gupta, S., Raden, D.L., and Davis, R.J. 1992. Signal transduction within the nucleus by mitogen-activated protein kinase. *J. Biol. Chem.* **267**:24796–24804.
56. Demicco, E.G., et al. 2005. RelB/p52 NF-kappaB complexes rescue an early delay in mammary gland development in transgenic mice with targeted superrepressor IkappaB-alpha expression and promote carcinogenesis of the mammary gland. *Mol. Cell. Biol.* **25**:10136–10147.
57. Coudronniere, N., Villalba, M., Englund, N., and Altman, A. 2000. NF-kappa B activation induced by T cell receptor/CD28 costimulation is mediated by protein kinase C-theta. *Proc. Natl. Acad. Sci. U. S. A.* **97**:3394–3399.
58. Hanstein, B., Liu, H., Yancisin, M.C., and Brown, M. 1999. Functional analysis of a novel estrogen receptor-beta isoform. *Mol. Endocrinol.* **13**:129–137.
59. Tran, H., et al. 2002. DNA repair pathway stimulated by the forkhead transcription factor FOXO3a through the Gadd45 protein. *Science.* **296**:530–534.
60. Pianetti, S., Arsura, M., Romieu-Mourez, R., Coffey, R.J., and Sonenshein, G.E. 2001. Her-2/neu overexpression induces NF-kappaB via a PI3-kinase/Akt pathway involving calpain-mediated degradation of IkappaB-alpha that can be inhibited by the tumor suppressor PTEN. *Oncogene.* **20**:1287–1299.
61. Brunet, A., et al. 2001. Protein kinase SGK mediates survival signals by phosphorylating the forkhead transcription factor FKHRL1 (FOXO3a). *Mol. Cell. Biol.* **21**:952–965.
62. Srivastava, K.K., et al. 2004. Engagement of protein kinase C-theta in interferon signaling in T-cells. *J. Biol. Chem.* **279**:29911–29920.